Mine Water Environ (2010) 29:53–67
DOI 10.1007/s10230-010-0099-z

TECHNICAL ARTICLE

Evaluation of Metal Attenuation from Mine Tailings in SE Spain (Sierra Almagrera): A Soil-Leaching Column Study

A. Navarro Flores · F. Martínez Sola

Received: 19 May 2009 / Accepted: 21 January 2010

Abstract A laboratory study was undertaken using mine tailings and soil columns to evaluate some of the natural processes that can control the mobility of metals at Pb–Ag mine tailings impoundments. The effects of buffering, pH, and salinity were examined with tailings from the El Arteal deposit. Al, Ba, Cd, Cu, Fe, Mn, Ni, Pb, Sr, and Zn were mobilized when the tailings were leached. However, when the mine tailings were placed above alluvial soils, Al, Ba, Cd, Cu, Mn, Pb, and Zn were retained, although Fe and Sr clearly remained mobile. Most of the metal retention appears to be associated with the increase in pH caused by calcite dissolution. The sorption of some metals (Cu, Pb, and Zn) onto oxyhydroxides of Fe and Mn, sulphates, clay materials, and organic matter may also explain the removal of these metals from the leachate.

Keywords Leaching · Metals · Mine sites · Soils · Tailings

Introduction

Mining in southeastern Spain dates back to the third millennium BC (Almagro Gorbea 1970). Most exploitation occurred between 1838 and 1991, and focused on the mining of Pb–Zn–Fe deposits in Sierra de Cartagena (Oen et al. 1975), the Pb–Ag (Fe, Ba) vein deposits in Sierra Almagrera (Navarro et al. 2004), the Pb–Zn–Ag vein deposits in Mazarrón, and the Au–Ag epithermal deposits in Rodalquilar (Arribas et al. 1995). Metal mining has ceased, but there are hundreds of abandoned mine sites located near urban and agricultural areas. The mine waste, tailings, and metallurgical waste have contaminated soil, sediments, and ground water (Moreno et al. 2007; Navarro et al. 2000, 2004, Navarro et al. 2008; Robles-Arenas et al. 2006; Wray 1998).

The remediation of metal-contaminated sites is possible by means of a variety of acid neutralization and metal removal treatments based on the use of alkaline materials such as limestone (Cravotta and Watzlaf 2002; Nicholson et al. 1988, 1990; Younger et al. 2002). Other materials that have been used include alkaline tailings, fly ash, red mud, quicklime (CaO), portlandite ($Ca(OH)_2$), calcium peroxide (CaO_2), dolomite ($CaMg(CO_3)_2$), magnesite ($MgCO_3$), caustic magnesia (MgO), witherite ($BaCO_3$), hydroxyapatite ($Ca_5(PO_4)_3OH$), sodium orthosilicate (Na_4SiO_4), and waste materials (Basta and McGowen 2004; Kumpiene et al. 2007; McCullough et al. 2008; Navarro and Martínez 2008; Navarro et al. 2006a, b; Pérez-López et al. 2007; Sneddon et al. 2006). Column and pilot-scale experiments (Alakangas and Öhlander 2006; Hulshof et al. 2006; Yanful et al. 1999) have been conducted on the application of soil covers and reactive layers to control acid mine drainage (AMD).

Besides these remediation measures, monitored natural attenuation (MNA), applied in conjunction with other cleanup approaches, may be an acceptable treatment option. Natural attenuation processes include physical, chemical, and biological processes that can reduce the mass, concentration, and mobility of contaminants, such as neutralization, adsorption, and mineral precipitation (Wilkin 2008). The application of MNA to inorganic

A. Navarro Flores (✉)
Dept M Fluidos, ETSEIAT, Univ Politécnica de Cataluña (UPC), Colón, 7, 08222 Terrassa, Spain
e-mail: navarro@mf.upc.edu

F. Martínez Sola
Deretil SA, Villaricos, 04618 Cuevas del Almanzora, Almería, Spain

contaminants requires the demonstration of contaminant sequestration mechanisms and estimation of attenuation rates and attenuation capacity of aquifer solids (EPA 2007). A primary control on the process of metal attenuation is acid neutralization; thus, water that drains carbonate-rich waste dumps or materials of high neutralization capacity tends to have near-neutral pH values (5.7–7), though it may contain moderate amounts of Pb, Cd, and As, and high concentrations of Cu, Ni, and Zn (Balistrieri et al. 2002; Blowes et al. 1998; Heikkinen et al. 2009; Kovács et al. 2006; Plumlee et al. 1999).

Mining of polymetallic ore deposits similar to the Sierra Almagrera deposits produces Pb–Zn flotation tailings that generate leachates with high amounts of sulfate (280–29,500 mg/L), As (<0.01–12 mg/L), Fe (0.025–2,352 mg/L), Mn (0.1–732 mg/L), Zn (<0.025–1,465 mg/L), and Pb (<0.01–0.351 mg/L) (Talavera et al. 2006). Secondary phases such as gypsum, goethite, hematite, and jarosite precipitate, which attenuates the concentrations of Zn, Cd, Cu, and As (Romero et al. 2007). At these sites, Pb is the contaminant of greatest concern, although its mobility is limited due to Pb sorption by hydrous ferric oxides and the possible precipitation of secondary phases such as plumbojarosite (Frau et al. 2008). Under these conditions, the impact on ground water can be considerable, even when carbonate rocks neutralize the AMD, greatly increasing the amount of dissolved and suspended metals (Cidu et al. 2008).

At tailings and waste rock impoundments in semi-arid environments, like the study area, the precipitation of secondary minerals due to solubility limits or neutralization can be another important metal attenuation mechanism (Smuda et al. 2007). The most common secondary minerals are goethite, jarosite, gypsum, and efflorescent salts in sulfide-rich impoundments. The accumulation of trace metals by adsorption and co-precipitation with Fe oxyhydroxides can serve as a larger sink for many metals. These secondary products from the pH-buffering and sulfide oxidation reactions can accumulate at depth, sometimes forming ‘hardpans’ or cemented layers. Furthermore, the dissolution of efflorescent salts during rain events can cause the formation of acid solutions rich in Fe, Mn, Zn, Cu, Cd, As, and S (Jambor et al. 2000; Smuda et al. 2007). Also, the extent of the Fe/Mn/Al oxide fraction of soils in the retention of contaminants may explain the high concentration of trace elements associated with this fraction (Dybowska et al. 2006).

The first objective of this study was to characterize the uncontrolled mine tailings of the Pb-Ag El Arteal deposit in Almería (SE Spain). Water samples collected in laboratory column experiments permitted the controlled collection of leaching data and the temporal evaluation of dissolved metals. A second objective was to evaluate whether natural attenuation processes in the Sierra Almagrera mining area soils might control the mobility of metals released from the El Arteal mine tailings.

Materials and Methods

Study Area

The study area has a semi-arid climate with an average annual precipitation of 200 mm and an ephemeral surface runoff, which can be considerable since 50% of the annual precipitation may fall in several days. The Sierra Almagrera mining district is located along the eastern border of the Betic Cordillera, which is the central part of a wide volcano-tectonic and metallogenic belt that extends from Cabo de Gata to Sierra de Cartagena. In the study area, the Almanzora river basin (1,800 km^2) runs across a tectonic basin between two metamorphic ranges: Sierra Almagrera and Sierra de Almagro. It is filled with Tertiary deposits and covered with Quaternary alluvial and deltaic deposits from the Almanzora River. The uncontrolled accumulation of tailings in the El Arteal deposit (3,500,000 t), the Jaravías deposit (300,000 t), the Herrerías impoundments, and several smelter slag dumping areas (Navarro and Martínez 2008; Navarro et al. 2008, all pose a high environmental risk.

The mineral vein deposits mined in the Sierra Almagrera are mainly made up of galena, barite, siderite, and Ag–Pb sulfosalts. In the nineteenth century, about 45 polymetallic veins (0.15–7 m thick) were exploited down to 180 m below sea level, which was the maximum depth allowed by the ground water pumping system available. Mining declined in the early twentieth century and was discontinued at the beginning of the Spanish Civil War. Selective underground mining (high-grade lead-silver veins) was reinitiated in 1945 by the state-owned company MASA (Minas de Almagrera, S.A.) and ceased in 1957, when the exploitation level reached 220 m below sea level and mining costs increased dramatically. From 1967 to 1991, the workings focused on processing low-grade stockpiles, which resulted in sand and silt-sized tailings from the El Arteal deposit. The ore was extracted by crushing, grinding and flotation using sodium ethyl xanthate.

The tailings were dumped in an unconfined aquifer formed by the alluvial terraces of the Canalejas River, the main tributary of the Almanzora River. These sedimentary deposits are a Quaternary formation that has built up over an impermeable clayey Miocene platform and the metamorphic basement. The base layers of the deposit are gravel and fine sand; sand layers and silts dominate the upper part. The Almanzora aquifer in the study area is 25–40 m thick, with a saturated thickness of $\approx$ 7 m. The water table is generally located 20–30 m below the surface, with annual and seasonal oscillations (Navarro et al. 2004).

Sample Collection and Analysis

Six samples of representative mineralization and 20 samples of mine wastes were collected, along with 13 samples of tailings and 30 samples of contaminated soils and sediments from a depth of approximately 0–0.25 m (Fig. 1). The samples were crushed to less than 10 mesh in a jaw crusher, quartered, pulverized in an agate mortar, re-homogenized, and repacked in plastic bags. The tailings, sediments, and soil samples were sent to Actlabs (Ontario, Canada). Au, Ag, As, Ba, Br, Ca, Ce, Co, Cr, Cs, Eu, Fe, Hf, Hg, Ir, La, Lu, Na, Ni, Nd, Rb, Sb, Sc, Se, Sm, Sn, Sr, Ta, Th, Tb, U, W, Y and Yb were quantitatively analyzed by instrumental neutron activation analysis (INAA), and Mo, Cu, Pb, Zn, Ag, Ni, Mn, Sr, Cd, Bi, V, Ca, P, Mg, Tl, Al, K, Y and Be were analyzed by inductively coupled plasma emission spectroscopy (ICP-OES).

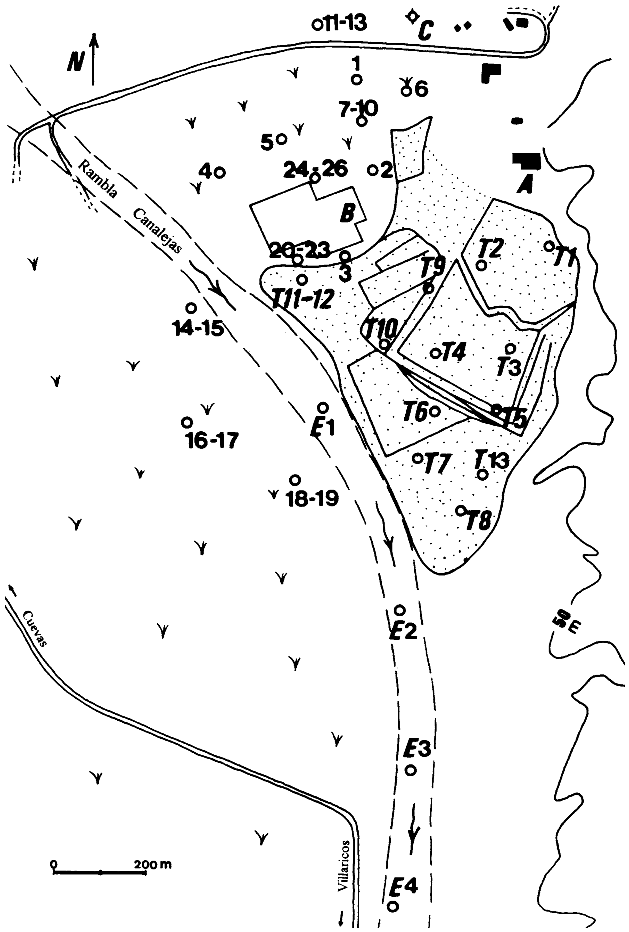

Fig. 1 Location of sediment, soil and tailing samples; *A* old flotation plant, *B* old miner housing, *C* well pumping system; *T1–T13* tailing samples, *1–26* soil samples, *E1–E4* sediment samples; *shaded area* location of mine tailings

Mine waste, mineralization, sediments, and soil samples were studied using binocular microscopy, transmitted and reflected light microscopy, and X-ray diffraction (XRD). These techniques enabled us to identify the mineral phases and subsequently analyze the major and trace element contents of the most abundant minerals.

Shallow, non-contaminated soils were collected from the alluvial deposits of the Almanzora River, upstream of the main dumping area (El Arteal). Particle size analysis was determined using an analytical sieve shaker (Retsch AS 200 model). Hydraulic conductivity and effective porosity were determined, respectively, with a constant-head permeameter and by water displacement in a test tube. Soil electrical conductivity was determined using a conductivity meter (Hach sensION5) on the saturation extract; soil pH values were measured using glass electrodes in a soil:water ratio of 1:2.5; CaCO3 content was determined by titration; organic carbon was determined by the wet combustion method; and cation exchange capacities (CEC) were determined using the Breeuwsma equation (Breeuwsma et al. 1986).

Column Experiments

The column experiments were performed using an experimental setup that consisted of a water reservoir, a peristaltic pump, a methacrylate column (0.75 m length and 0.15 m diameter), and a series of instruments to determine a number of the parameters of the effluents in situ, such as pH, Eh, electrical conductivity, temperature, and dissolved O_2 (Navarro and Martínez 2008; Navarro et al. 2008).

Low mineralized water (LMW) entered the columns through an injection system connected to a metering pump. A constant-head reservoir was used to deliver influent water at a flow rate of 1.0 $L \cdot h^{-1}$. The solids used in the experiments were moderately oxidized tailings collected at the main impoundment of the El Arteal deposit (Fig. 1). The experiments comprised:

1. Leaching of pure tailings with LMW.
2. Leaching of 0.1 m of tailings above 0.6 m of alluvial soil with LMW.
3. Leaching of 0.1 m of tailings above 0.6 m of alluvial soil with LMW containing 5 g/L of NaCl.
4. Leaching of 0.1 m of tailings above 0.6 m of alluvial soil with LMW acidified with HNO_3 ultrapure until pH < 2.

The samples were collected at the bottom of the column as a function of time. The first sample, corresponding to time 0, was taken when water started to flow from the lower part of the column. Flow, pH, and EC were measured immediately after sample collection.

The pH, temperature and EC (µS/cm), corrected using standard solutions, were measured in situ using portable devices (HACH sensION378). The samples were filtered using a cellulose nitrate membrane with a pore size of 0.45 µm. The samples for cation analysis were later acidified to $pH < 2.0$ by adding ultra-pure HNO_3. The samples were collected in 110 ml high-density polypropylene bottles, sealed with a double cap, and stored in a refrigerator until analyzed. The metal concentrations were measured using inductively coupled plasma mass spectroscopy (ICP-MS) and ICP-OES at Barcelona University.

Hydrodynamic dispersion coefficients and dispersivity were determined in the laboratory using columns packed with the alluvial soils under investigation. They were subjected to the continuous injection of a chloride solution in a uniform flow field from a single point located at the top of the columns. The results obtained, in terms of the relative concentration of chloride against the pore volumes of fluid eluted, were analyzed using the analytical solution to advection–dispersion derived from Ogata and Banks (1961). The immobilization/attenuation of metals by alluvial soils was evaluated by comparing the leachates obtained in the soil-leaching experiments with the metal leaching from the column experiment with pure mine tailings.

Hydrogeochemical analyses of leachates were performed using the PHREEQC numerical code (Parkhurst and Appelo 1999) to evaluate the speciation of dissolved constituents and calculate the saturation state of the effluents. The MINTEQ thermodynamic database was used for the chemical equilibrium calculations. The total concentrations of metals and other elements were used in the geochemical modeling. PHREEQC was applied to the column solution compositions in order to provide a basis for interpreting the inverse model, which was also used to analyze the solubility controlling minerals. Redox potentials (Eh, mV) were measured with a portable device equipped with a platinum electrode. These data were used to define redox speciation in the geochemical modeling.

Results and Discussion

Mine Waste Mineralogy and Geochemistry

X-ray diffraction (XRD) analysis and binocular microscope analysis showed the mineralogy of the tailings to be dominated by quartz (6–48%), clay minerals (24–49%), barite (3–10%), galena (5%), gypsum (2–3%), and carbonates (0.5%) (Table 1). A portion of the tailings is derived from the vein deposits, but most is derived from the processing of low-grade stockpiles between 1969 and 1991. Moreover, the XRD data indicated the presence of cinnabar, canfieldite, gersdorsfite and smithite as primary phases, and goethite, hercynite, kaolinite, argentojarosite, gypsum, jarosite, hidroniojarosite, natroalunite, langite, bonattite, ferrohexahydrite, and szomolnokite as secondary phases (Table 1). The mine wastes obtained in the main exploitation areas (the Jaroso and Francés ravines) showed the presence of quartz, barite, galena, siderite, chalcopyrite, arsenian pyrite, sphalerite, and muscovite as main primary phases, and goethite, hematite, anglesite, nantokite, calcite, kaolinite, and natroalunite as secondary phases (Table 2).

Table 1 Mineralogy of the tailings in El Arteal deposit

Mineral phases	Formula
Primary phase	
Galena	PbS
Barite	$BaSO_4$
Cinnabar	HgS
Canfieldite	Ag_8SnS_6
Gersdorsfite	$NiAsS$
Quartz	SiO_2
Calcite	$CaCO_3$
Siderite	$FeCO_3$
Smithite	$(Ag, Cu)_{16}Sb_2S_{11}$
Secondary phase (low solubility)	
Goethite	$FeOOH$
Hercinite	$FeAl_2\ O_4$
Kaolinite	$Al_4(Si_4O_{10})\ (OH)_8$
Secondary phase (low-solubility sulfate minerals)	
Argentojarosite	$Ag_2Fe_6(SO_4)_4(OH)_{12}$
Gypsum	$Ca(SO_4)\cdot 2H_2O$
Jarosite	$KFe_3(SO4)_2(OH)6$
Hidroniojarosite	$(H3O)_3\ Fe_3\ (SO4)_2(OH)_6$
Natroalunite	$NaAl_3(SO_4)_2(OH)_6$
Langite	$Cu4(SO_4)(OH)6\cdot 2H_2O$
Secondary phase (medium/high-solubility sulfate minerals)	
Bonattite	$Cu(SO_4)\cdot 3H_2O$
Goldichite	$KFe(SO_4)_2\cdot 4H_2O$
Ferrohexahydrite	$FeSO_4\cdot 6H_2O$
Szomolnokite	$FeSO_4\cdot H_2O$

Analysis of the uncontrolled tailings of El Arteal (SA) showed high amounts of Ag (26.6 ppm), As (278.4 ppm), Ba (5.8 wt%), Cu (59.0 ppm), Pb (2879.3 ppm), Sb (169.8 ppm), and Zn (2179.2 ppm). These levels are above the metal contents for contaminant soil allowed by law (Table 3). The contaminants of greatest environmental concern are As and Pb, which show a mean concentration of 278.4 and 2879.3 ppm, respectively. In the tailings, the concentrations rise to 460 and 5,428 ppm, respectively. The values detected in the soils and sediments surrounding the tailings impoundment, which is an area of intense agricultural activity, are 340 and 3,244 ppm, respectively.

Table 2 Identified phase minerals in Sierra Almagrera mining wastes impoundments

Mineral phases	Formula
Quartz[a]	SiO_2
Galena[a]	PbS
Barium strontium sulfate[a]	$Ba_{0.75}\cdot Sr_{0.25}\cdot SO_4$
Siderite[a]	$FeCO_3$
Arsenian pyrite	$Fe(S_{1-x}As_x)_2$
Muscovite	$Al_{2.9}H_2KO_{12}Si_{3.1}$
Nantokite	CuCl
Anglesite	$PbSO_4$
Sphalerite	ZnS
Periclase	MgO
Oyelite	$(CaO)\cdot SiO_2\cdot zH_2O$
Chalcopyrite	$CuFeS_2$
Wuestite	FeO
Calcite	$CaCO_3$
Anorthite	$Ca(A_{l2}Si_2O_8)$
Natroalunite	$NaAl_3\ (SO_4)_2\cdot (OH)_6$
Hematite	Fe_2O_3
Kaolinite	$Al_4(Si_4O_{10})\cdot (OH)_8$

[a] High-abundance phase

The high levels of As may be due to the arsenopyrite associated with the ore (Table 3), and, possibly, weathering crusts of ferric oxides and Fe-oxyhydroxides (Moreno et al. 2007). During weathering, the As substituted within the pyrite may enhance the rate of oxidation and dissolution, which liberates As and other pollutants; these spread to pore water and seeps that flow from the tailings in wet periods. The higher content of As in the mine wastes may reflect a high percentage of arsenopyrite and other As-minerals at these dump sites.

There are also high concentrations of Pb in the mine wastes, tailings, and soils and sediment (mean concentrations of 12773.8, 2879.3, and 1642.1 ppm, respectively), due mainly to the presence of galena (Table 3).

Copper, silver, and cadmium occur in moderate concentrations in the tailings (mean concentrations of 59, 26.6, and 17.6 ppm, respectively) and the soils and sediment (43.4, 6.7, and 1.7 ppm, respectively) due to the presence of chalcopyrite, silver rich-galena, and sphalerite in the processed ore (Table 3).

Antimony occurs in high concentrations in the tailings (mean: 169.8 ppm) and the soils and sediment (mean: 69.2 ppm). In the mine wastes, the Sb concentrations rose to 84,000 ppm and reached mean concentrations of 799.5 ppm. The primary Sb minerals are boulangerite, tetrahedrite, and antimony-rich galena, which are associated with vein deposits. Zinc shows above-average concentrations in the tailings (2179.2 ppm) and the soils and sediment (522.1 ppm) due to the presence of sphalerite.

Main Characteristics of the Soils

The alluvial soils used in the leaching column experiments had a low concentration of metals and metalloids (Table 3). Furthermore, the soils comprised 58.2% sandy material, with a moderate content of clay and silt. The CEC and organic carbon content were 2.7 and 0.25%, respectively (Table 4). The hydraulic conductivity obtained using the permeameter was 4.6 m/day, and the longitudinal hydrodynamic dispersion and dispersivity were 0.0186 cm^2/s and 2.65 cm, respectively, in concordance with experiments on similar materials (Silliman and Simpson 1987). Moreover, the dispersivity values are lower than the length and diameter of the leaching columns, which shows the correct dimensioning of the experiments (Navarro et al. 2006a, b).

The XRD of the reactive soils showed the presence of quartz, feldspars, hematite, calcite, dolomite, gypsum, and possible clay minerals (illite and chlorite). We also detected minor quantities of: acanthite, anglesite, argentojarosite, bornite, chalcanthite, halothrichite, hexahydrite, jamesonite, orpiment, thenardite, and zincosite.

Column Experiments

Solubility Controls on Dissolved Constituents

Column experiments were conducted to study the metal attenuation processes since, under controlled laboratory conditions, it was possible to eliminate unknown influences that could affect the geochemical evolution of pore water (Jurjovec et al. 2002). The characteristics of the leaching column experiments are shown in Table 5.

The first column experiment was conducted to simulate the effect of precipitation on the tailings impoundments. Measurements of effluent leachate pH during the pure-tailings experiment showed a pH close to 5.5–6, while the soil-column experiments showed an increase in pH to 7.40–8.20 (Fig. 2). Al, Ba, Cd, Cu, Fe, Mn, Ni, Pb, Sr, and Zn were mobilized in the pure-tailings column experiment (Table 6).

Major Ions

Sulfate was the dominant anion in the leaching experiments, reaching a maximum dissolved concentration of 2,600 mg/L, due to sulfide oxidation and the thermal water used in the flotation process. Bicarbonate reached concentrations of 129.7 mg/L in the soil leached with LMW, 107.9 mg/L in the soil leached with a saline solution, and 226.1 mg/L in the soil leached with an acidic solution.

Table 3 Concentrations of metals and metalloids in mine waste of El Arteal deposit and nearby soils at Sierra Almagrera (Almería)

	Au	Ag	As	Ba	Cd	Cu	Hg	Fe	Pb	Se	Sb	Zn
Mining wastes												
Mean	91.2	59.2	4,885	6.8	37.2	5497.5	9.9	19.7	12733.8	23.9	4233.2	7995
Min	<2	0.4	<0.5	<0.2	<0.5	6	<1	1.57	33	<3	37	18
Max	827	457.7	86,000	39	305.4	64,391	180	51	40,375	470	84,000	100,000
Tailings												
T1	15	46	460	3.2	NA	NA	<1	15.4	NA	<5	270	2,270
T2	10	25	260	6.3	NA	NA	<1	13.3	NA	<5	120	2,460
T3	<5	27	270	8.5	NA	NA	<1	12.7	NA	<5	180	2,550
T4	<5	33	330	4.6	NA	NA	2	12.4	NA	<5	200	2,170
T5	<5	25	200	4.6	NA	NA	<1	10.4	NA	<5	130	1,870
T6	<5	15	210	5.4	NA	NA	<1	11.8	NA	<5	120	1,600
T7	<5	40	410	4.0	NA	NA	<1	12.5	NA	<5	270	1,520
T8	<5	39	270	4.0	NA	NA	<1	11.7	NA	<5	260	2,000
T9	<5	28	260	5.3	NA	NA	<1	13.1	NA	<5	110	2,620
T10	<5	26	250	6.1	NA	NA	3	13.2	NA	<5	200	2,280
T11	<2	8	230	5.3	35	21	<1	10.0	1,622	<3	82	1,790
T12	<2	9	220	10.0	12	22	3	12.0	1,588	<3	66	3,000
T13	<2	25	250	8.1	5.8	134	<1	13.1	5,428	<3	200	2,200
Mean	–	26.6	278.4	5.8	17.6	59.0	–	12.4	2879.3	–	169.8	2179.2
Min	<2	5.0	200	3.2	5.8	21.0	<1	10.0	1588.0	<3	66.0	1520.0
Max	15	46.0	460	10.0	35.0	134.0	3.0	15.4	5428.0	<5	270.0	3000.0
TSL	<2	27.5	265	4.9	5.8	27.5	<1	13.1	1,881	<3	190	2,220
Soils and sediments												
1	<5	<5	110	1.0	NA	NA	<1	6.52	NA	<5	92	444
2	<5	15	99	1.6	NA	NA	<1	6.11	NA	<5	92	600
3	<5	12	48	1.0	NA	NA	<1	5.69	NA	<5	40	375
4	<5	9	56	1.0	NA	NA	<1	5.57	NA	<5	61	572
5	<5	9	62	0.2	NA	NA	<1	4.79	NA	<5	48	220
6	6	40	340	2.5	NA	NA	<1	10.2	NA	<5	330	1,180
7	26	13	123	1.2	2.1	65	1	5.77	3,219	<3	98	560
8	12	12	117	1.2	2.1	64	<1	6.07	3,161	<3	109	543
9	21	12	109	1.2	2	56	<1	6.24	2,990	<3	104	523
10	9	12	146	1.2	0.9	44	<1	7.07	3,244	<3	94.4	391
11	12	10	74	0.54	2.3	69	<1	5.05	2,131	<3	76.7	623
12	19	11	63.4	0.59	2.1	66	<1	5.37	2,085	<3	78.7	677
13	7	8	70.5	0.41	1.4	58	2	5.09	1,642	<3	74.6	521
14	<2	<5	32.4	0.26	0.6	28	<1	4.13	599	<3	28.9	351
15	11	<5	38.9	0.25	0.8	32	<1	4.32	703	<3	29.7	283
16	12	<5	24	0.06	0.5	27	<1	4.37	166	<3	9.1	150
17	9	<5	25.4	0.07	0.06	27	<1	4.42	257	<3	13	140
18	12	<5	18	0.09	0.5	30	<1	4.01	152	<3	6.5	141
19	7	<5	19.9	0.08	0.5	27	<1	4.13	183	<3	8	135
20	2	8	49	1.8	3.4	30	<1	6.36	1,156	<3	53	532
21	9	8	52	1.7	3.5	35	<1	6.99	1,234	<3	61	513
22	4	6	41	1.3	2.6	28	<1	5.45	1,029	<3	50	469
23	<2	<5	46	1.6	2.3	29	<1	5.41	1,110	<3	37	584
24	<2	11	92	1.5	3.5	53	<1	5.43	2,522	<3	71	648
25	8	15	92	0.44	1.8	60	<1	5.14	3,168	<3	90	360

Table 3 continued

	Au	Ag	As	Ba	Cd	Cu	Hg	Fe	Pb	Se	Sb	Zn
26	9	10	80	0.33	1.2	41	<1	5.15	2,092	<3	60	220
E1	<5	23	210	3.0	NA	NA	<1	9.39	NA	<5	150	2,000
E2	6	7	56	0.82	NA	NA	<1	5	NA	<5	46	678
E3	10	<5	68	0.65	NA	NA	<1	5.7	NA	<5	47	850
E4	<5	<5	32	0.23	NA	NA	<1	4.8	NA	<5	19	380
Mean	8.2	6.7	79.8	0.9	1.7	43.4	–	5.6	1642.1	–	69.2	522.1
Min	<2	<5	18	0.06	0.06	27	<1	4.0	152	<3	6.5	135
Max	26	40	340	3.0	3.5	69	2.0	10.2	3,244	<5	330	2,000
SLE	<5	<5	12.2	0.024	<0.06	9	<1	3.59	12	<3	2.8	81
NH	–	15[a]	55	0.0625	12	190	10	–	530	100[a]	15	720

Values in ppm except Ba and Fe (%) and Au (μg kg^{-1}). *T* tailings samples, *E* sediments, *TSL* tailings sample used in the leaching tests, *SLE* alluvial soil used in the soil-leaching column experiments, *NH* The Netherlands soil intervention values, *NA* not analyzed. [a] indicative levels of serious contamination

Table 4 Main characteristics of alluvial soils used in the column-leaching tests

Grain size (%)	ε	Organic C (%)	CEC (meq/100 g)	K (m/day)	EC (μS/cm)	pH	DL (cm2/s)	A (cm)
Gravel: 36.2 Sand: 58.2 Silt: 2.9 Clay: 2.7	0.29	0.25	2.76	4.64	850	9.19	0.0186	2.65

ε, Porosity; K, hydraulic conductivity; EC, electrical conductivity; DL, longitudinal hydrodynamic dispersion; α, dispersivity

Table 5 Characteristics of leaching column experiments

Experiment	L (m)	D (m)	Porosity
TL	0.75	0.15	0.05
SS	0.75	0.15	0.29

TL leaching of mine wastes only, *SS* soil-column experiments (3), *L* column length, *D* column diameter

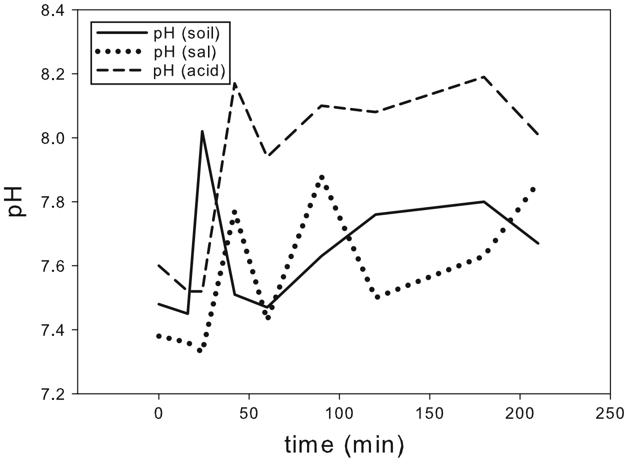

Fig. 2 Changes in pH in the leaching tests; *pH(soil)* leaching of mine waste and alluvial soil with LMW (low mineralized water), *pH(sal)* leaching of mine waste and alluvial soil with saline water, *pH(acid)* leaching of mine waste and alluvial soil with acidic water

Calcium, K, Mg, Na, and Si may be released to the tailings pore-water as represented by the tailings leachate due to aluminosilicate mineral dissolution. Calcium and Mg may also be released by calcite, dolomite, and gypsum dissolution. The concentration of Ca greatly increased in the soil-column experiments (Fig. 3) (to >300 mg/L), more than double the detected concentrations in the pure tailings leachate (100–120 mg/L). This increase is most likely a result of carbonate dissolution, because the pH (Fig. 2) indicates a possible buffering effect; the soil contains >12% carbonates. Moreover, the release of Ca to the leachate increased in the experiment with saline water, reaching concentrations of 900 mg/L, which may indicate that cation exchange is occurring between Na^+ and Ca^{2+} in the soil. The buffering role of the soil was also evident in the acidic experiment, which showed pH values around 8 (Fig. 2), and the possible release of Ca (Fig. 3).

Metals

Al, Ba, Cd, Cu, Fe, Mn, Ni, Pb, Sr, and Zn were released in the pure-tailings experiment, several at concentrations significantly above the European Drinking Water Standards (EDWS) (Table 6). Most of the soluble secondary phases

Table 6 Concentrations of metals and metalloids of pure-tailings column experiment

Element	m.01a	m.02a	m.03a	m.04a	m.05a	m.06a	m.07a	m.08a	m.09a	m.10a	m.11a	m.12a
Ag (ppb)	<1.00	<1.00	<1.00	<1.00	<1.00	<1.00	<1.00	<1.00	<1.00	<1.00	<1.00	<1.00
As (ppb)	<5.00	<5.00	<5.00	<5.00	<5.00	<5.00	<5.00	<5.00	<5.00	<5.00	<5.00	<5.00
Cd (ppb)	23.46	26.74	24.26	20.62	19.33	17.12	13.37	11.49	10.82	11.12	10.09	7.98
Cu (ppb)	31.12	24.93	15.39	11.89	9.19	11.51	29.23	22.47	17.52	15.41	15.17	14.56
Cr (ppb)	2.45	2.19	1.60	1.38	1.25	1.34	1.25	1.60	1.36	1.24	1.12	1.38
Mo (ppb)	<0.50	<0.50	<0.50	<0.50	<0.50	<0.50	<0.50	<0.50	<0.50	<0.50	<0.50	<0.50
Ni (ppb)	29.67	33.33	24.19	21.57	16.83	20.95	13.19	12.36	12.05	9.38	9.08	10.66
Sb (ppb)	<1.00	<1.00	<1.00	<1.00	<1.00	<1.00	<1.00	<1.00	<1.00	<1.00	<1.00	<1.00
Zn (ppb)	902.28	724.71	623.60	529.80	467.84	446.01	353.56	305.54	305.49	275.50	252.62	207.48
Pb (ppb)	298.82	134.31	63.61	52.21	42.18	42.79	48.46	44.90	63.30	57.24	46.97	42.21
Co (ppb)	11.54	13.03	11.43	9.34	8.63	7.43	5.58	4.68	4.28	4.53	3.87	2.96
Au (ppb)	2.52	0.93	<0.50	<0.50	<0.50	<0.50	<0.50	3.17	<0.50	2.24	<0.50	<0.50
Hg (ppb)	<2.50	<2.50	<2.50	<2.50	<2.50	<2.50	<2.50	<2.50	<2.50	<2.50	<2.50	<2.50
Ba (ppm)	0.08	0.09	0.11	0.10	0.13	0.12	0.15	0.20	0.19	0.17	0.20	0.24
Fe (ppm)	0.86	0.53	0.30	0.21	0.15	0.12	0.12	0.09	0.12	0.24	0.07	0.10
Sr (ppm)	1.68	2.00	2.05	2.11	2.25	2.26	2.34	2.39	2.42	2.64	2.51	2.52
Si (ppm)	0.77	0.83	0.88	0.83	0.73	0.91	0.73	0.74	0.64	0.73	0.57	0.68
Ca (ppm)	118.73	129.51	121.66	114.90	114.93	110.97	105.17	102.36	100.23	110.39	97.75	87.88
Mg (ppm)	74.83	79.95	58.20	39.87	33.11	23.62	13.37	9.20	7.79	8.11	5.29	3.51
Mn(ppm)	8.60	10.41	9.06	7.44	6.62	5.58	3.87	3.06	2.72	2.75	2.26	1.50
K (ppm)	11.55	12.87	8.69	6.52	6.15	5.01	3.47	2.48	2.30	2.45	2.10	1.60
Al (ppm)	0.22	0.20	0.34	0.30	0.27	0.33	0.29	0.34	0.26	0.27	0.19	0.29
Na (ppm)	46.15	43.45	23.48	13.25	12.42	7.48	8.03	7.82	7.77	7.57	5.81	5.79

m01: 0 min, m02: 16 min, m03: 24 min, m04: 33 min, m05: 42 min, m06: 51 min, m07: 60 min, m08: 90 min, m09: 120 min, m10: 150 min, m11: 180 min, m12: 210 min

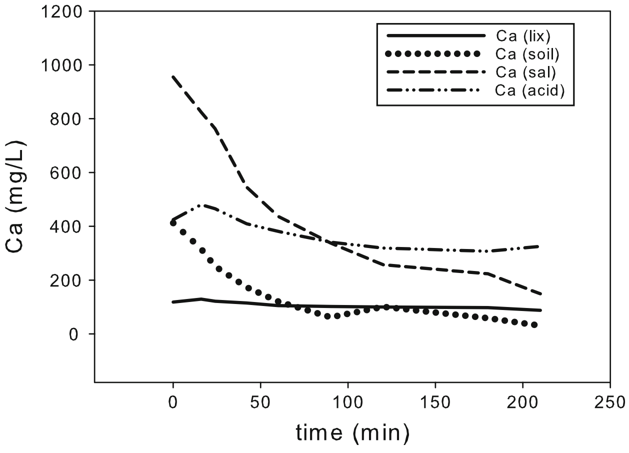

Fig. 3 Changes in Ca in the leaching tests; *Ca(lix)* leaching of pure tailings with LMW(low mineralized water), *Ca(soil)* leaching of mine waste and alluvial soil with LMW, *Ca(sal)* leaching of mine waste and alluvial soil with saline water, *Ca(acid)* leaching of mine waste and alluvial soil with acidic water

detected by X-ray powder diffraction (Table 1) suggest the mobilization of Fe, Cu, Pb, and Zn from these secondary phases. In addition, distilled water extracts from these tailings indicated that the extractions were saturated to supersaturated with calcite, dolomite, gypsum, jarosite, and iron oxyhydroxides (Navarro et al. 2004). Pore water saturation, with respect to jarosite, natrojarosite, and gypsum (Al et al. 2000; McGregor et al. 1998), and the possible mobilization of metals from oxyhydroxides and sulfates, have been detected in other tailings areas. Ribet et al. (1995) and Jurjovec et al. (2002) respectively showed that tailings Fe(III) oxyhydroxides were the source of Fe, Ni, Cu, Cr, and Co, and Zn, Ni, Co, Pb, and Cd.

However, Ag, As, Bi, Hg, Sb, Se V, and Au were not significantly mobilized in the eluates. The low mobilization of Ag, As, and Sb in the pure tailings column experiment is consistent with the minerals that were detected by X-ray, since we did not detect soluble secondary phases such as Fe-sulfoarsenates or valentinite, whose dissolution can lead to the mobilization of these elements.

In the soil column experiments, however, Al, Ba, Cd, Cu, Mn, Pb, and Zn were retained, although Fe and Sr clearly remained mobile. For example, the Al concentration remained below 20 µg/L during the soil-column experiments, with concentrations below 0.2 µg/L in the saline and acidic experiments (Fig. 4), clearly below the

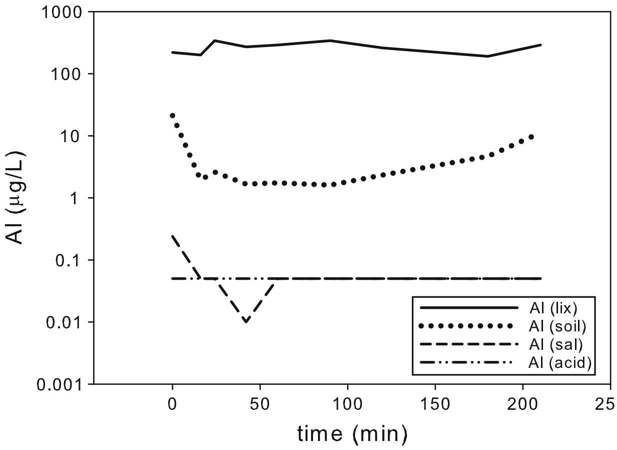

Fig. 4 Changes in Al in the leaching tests; *Al(lix)* leaching of pure tailings with LMW(low mineralized water), *Al(soil)* leaching of mine waste and alluvial soil with LMW, *Al(sal)* leaching of mine waste and alluvial soil with saline water, *Al(acid):* leaching of mine waste and alluvial soil with acidic water

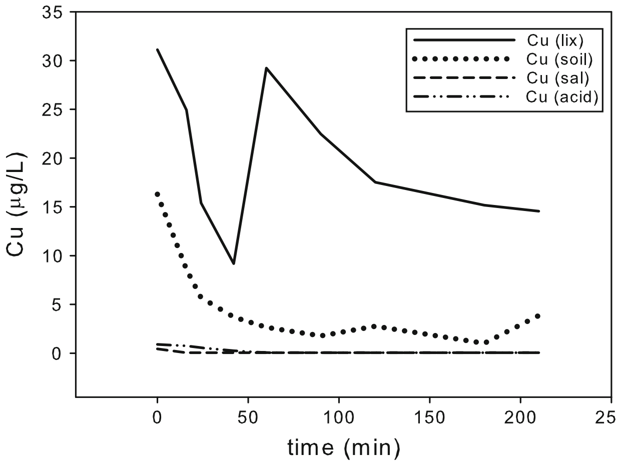

Fig. 6 Changes in Cu in the leaching tests; *Cu(lix)* leaching of pure tailings with LMW(low mineralized water), *Cu(soil)* leaching of mine waste and alluvial soil with LMW, *Cu(sal)* leaching of mine waste and alluvial soil with saline water, *Cu(acid)* leaching of mine waste and alluvial soil with acidic water

detected concentrations of the mine waste leachate (220–290 µg/L). The Al mobilization may be limited by gibbsite solubility (Jurjovec et al. 2002) or by the solubility of amorphous aluminium hydroxide, which is about 0.17 mg/L at pH 6.5.

The Ba concentrations in the soil column experiments were less than 100 µg/L (Fig. 5). The Cu concentrations were also very low in the soil experiments; only the leaching with LMW showed significant amounts of Cu, well below the Cu values of the tailings leachate (Fig. 6). At neutral to alkaline pH (>7) conditions, Cu oxides are stable, which probably explains the removal of this metal. In addition, chemical extraction tests suggest that Cu has a strong affinity for the surfaces of iron oxides and hydroxides (Ford et al. 2007).

Lead and Zn showed very limited mobility in the soil column experiments, even in the acidic experiments (Figs. 8, 9). At near-neutral to moderate alkaline pH, lead carbonates are stable, and hydrous ferric oxide, aluminium oxides, oxyhydroxides, and clay minerals can adsorb this metal (Dzomback and Morel 1990; Ford et al. 2007). The Mn concentrations were below 10 µg/L in the soil experiments compared to 8.6 mg/L in the tailings leachate (Fig. 7).

Among all of the metals, Fe had the highest concentrations in the soil experiment with LMW, reaching concentrations of 1.2 mg/L (Fig. 10), clearly above the

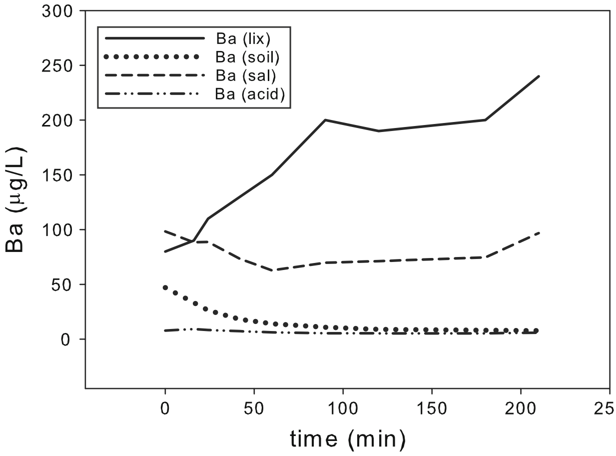

Fig. 5 Changes in Ba in the leaching tests; *Ba(lix)* leaching of pure tailings with LMW(low mineralized water), *Ba(soil)* leaching of mine waste and alluvial soil with LMW, *Ba(sal)* leaching of mine waste and alluvial soil with saline water, *Ba(acid)* leaching of mine waste and alluvial soil with acidic water

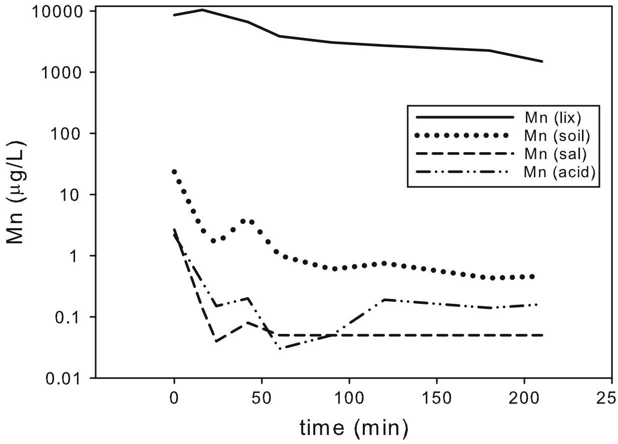

Fig. 7 Changes in Mn in the leaching tests; *Mn(lix)* leaching of pure tailings with LMW(low mineralized water), *Mn(soil)* leaching of mine waste and alluvial soil with LMW, *Mn(sal)* leaching of mine waste and alluvial soil with saline water, *Mn(acid)* leaching of mine waste and alluvial soil with acidic water

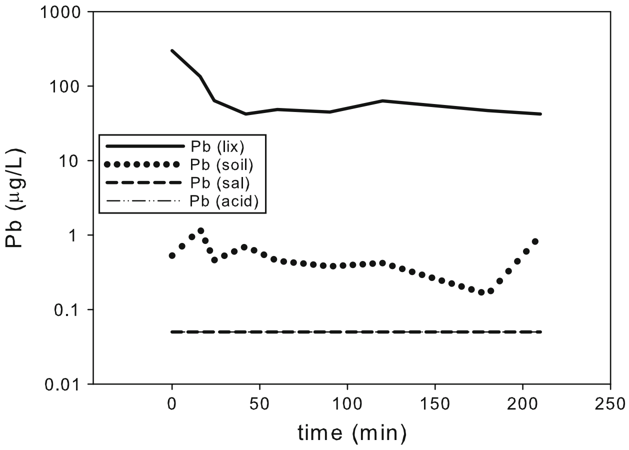

Fig. 8 Changes in Pb in the leaching tests; *Pb(lix)* leaching of pure tailings with LMW(low mineralized water), *Pb(soil)* leaching of mine waste and alluvial soil with LMW, *Pb(sal)* leaching of mine waste and alluvial soil with saline water, *Pb(acid)* leaching of mine waste and alluvial soil with acidic water

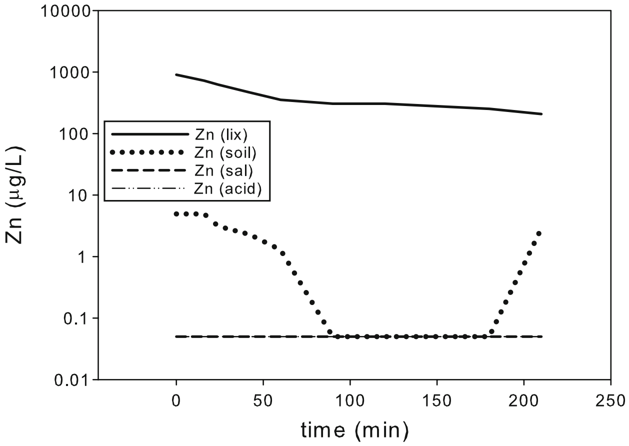

Fig. 9 Changes in Zn in the leaching tests; *Zn(lix)* leaching of pure tailings with LMW(low mineralized water), *Zn(soil)* leaching of mine waste and alluvial soil with LMW, *Zn(sal)* leaching of mine waste and alluvial soil with saline water, *Zn(acid)* leaching of mine waste and alluvial soil with acidic water

detected concentrations in the tailings leachate (0.86 mg/L). These elevated concentrations of Fe may be associated with the presence in the soil of Fe-soluble phases, such as halothrichite [$FeAl_2(SO_4)_4\cdot22H_2O$], and the Fe-minerals detected in the mine wastes (Table 1).

Geochemical Modeling

Calculations using PHREEQC for leachate speciation (Table 7) revealed that the most abundant species of Fe are Fe^{2+} and $FeSO_4$ in all the leachates, suggesting the mobilization of Fe from Fe(II) species such as melanterite and siderite. Similarly, the saturation index (Table 8) indicates that ferrihydrite, goethite, and jarosite were clearly saturated in the leachates, except in the leaching of mine wastes with LMW. Therefore, the possible mobilization of Fe may be caused by siderite dissolution and melanterite dissolution. Other possible sources of Fe indicated by the modeling include szomolnoquite, goldichite, and ferrohexahydrite, which were also detected by X-ray diffraction (Table 1). Furthermore, jarosite-H is undersaturated in all the leachates,

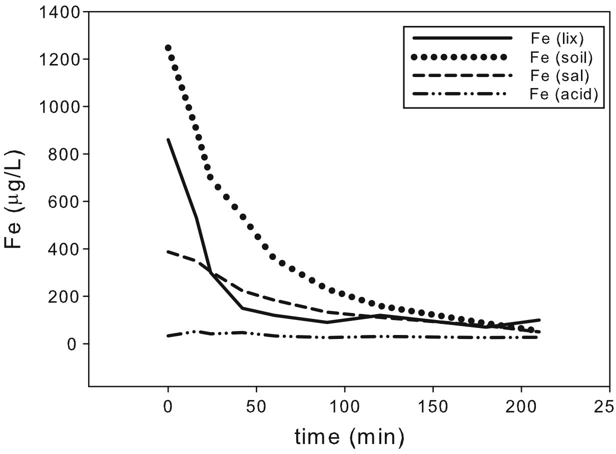

Fig. 10 Changes in Fe in the leaching tests; *Fe(lix)* leaching of pure tailings with LMW(low mineralized water), *Fe(soil)* leaching of mine waste and alluvial soil with LMW, *Fe(sal)* leaching of mine waste and alluvial soil with saline water, *Fe(acid)* leaching of mine waste and alluvial soil with acidic water

Table 7 Distribution of species for leachates; data calculated using PHREEQC and database MINTEQ, values in molality

Species	I	II	III	IV
Fe				
Fe^{2+}	$1.26\cdot10^{-5}$	$1.35\cdot10^{-5}$	$5.31\cdot10^{-6}$	$4.39\cdot10^{-7}$
$FeSO_4$	$2.74\cdot10^{-6}$	$7.24\cdot10^{-6}$	$1.33\cdot10^{-6}$	$1.12\cdot10^{-7}$
$Fe(OH)^{2+}$	$1.92\cdot10^{-8}$	$1.00\cdot10^{-6}$	$2.56\cdot10^{-7}$	$2.33\cdot10^{-8}$
Fe(OH)3	$6.23\cdot10^{-10}$	$2.80\cdot10^{-7}$	$5.16\cdot10^{-8}$	$9.02\cdot10^{-9}$
Mn				
Mn^{2+}	$1.26\cdot10^{-4}$	$2.67\cdot10^{-7}$	$2.59\cdot10^{-8}$	$2.84\cdot10^{-8}$
$MnSO_4$	$2.81\cdot10^{-5}$	$1.45\cdot10^{-7}$	$6.67\cdot10^{-9}$	$7.48\cdot10^{-9}$
Pb				
$PbCO_3$	$6.33\cdot10^{-7}$	$1.91\cdot10^{-9}$	$1.44\cdot10^{-10}$	$2.07\cdot10^{-10}$
Pb^{2+}	$3.43\cdot10^{-7}$	$1.29\cdot10^{-10}$	$2.55\cdot10^{-11}$	$1.13\cdot10^{-11}$
$PbSO_4$	$2.28\cdot10^{-7}$	$2.02\cdot10^{-10}$	$1.91\cdot10^{-11}$	$8.73\cdot10^{-12}$
Zn				
Zn^{2+}	$9.71\cdot10^{-6}$	$3.57\cdot10^{-8}$	$4.71\cdot10^{-9}$	$4.44\cdot10^{-9}$
$ZnSO_4$	$2.78\cdot10^{-6}$	$2.51\cdot10^{-8}$	$1.56\cdot10^{-9}$	$1.50\cdot10^{-9}$
$ZnCO_3$	$2.12\cdot10^{-7}$	$6.54\cdot10^{-9}$	$3.24\cdot10^{-10}$	$9.84\cdot10^{-10}$

I: leachate of pure tailings ($t = 0$), II: leachate of mine wastes and alluvial soil with LMW ($t = 0$), III: leachate of mine wastes and alluvial soil with saline solution ($t = 0$), IV: leachate of mine wastes and alluvial soil with acidic solution ($t = 0$)

Table 8 Calculated saturation index for leachates calculated using PHREEQC and database MINTEQ

Mineral phase	I	II	III	IV
Iron oxyhydroxides				
$Fe(OH)_3$	−0.49	2.16	1.44	0.67
Goethite	3.90	6.56	5.83	5.06
Mn minerals				
Pyrolusite	−13.39	−12.62	−13.95	−13.91
Rhodochrosite	−0.45	−2.19	−3.62	−3.09
Sulphate minerals				
Jarosite	−0.48	5.85	3.68	0.16
Jarosite-Na	−3.25	3.95	2.04	−2.18
Jarosite-H	−6.09	−0.93	−3.13	−6.69
Gypsum	−0.69	0.14	0.31	−0.07
Melanterite	−5.34	−4.92	−5.65	−6.73
Alunite	4.95	−1.15	−7.03	−7.46
Lead minerals				
Anglesite	−1.60	−4.64	−5.66	−6.01
Cerrusite	−0.31	−2.82	−3.93	−3.79
Zinc minerals				
Goslarite	−5.96	−8.01	−9.21	−9.23
Zincosite	−10.93	−12.97	−14.17	−14.20
Carbonate minerals				
$CaCO_3$	−1.11	0.26	0.33	0.44
$FeCO_3$	−1.31	−0.35	−1.17	−1.76

I: leachate of pure tailings ($t = 0$), II: leachate of mine wastes and alluvial soil with LMW ($t = 0$), III: leachate of mine wastes and alluvial soil with saline solution ($t = 0$), IV: leachate of mine wastes and alluvial soil with acidic solution ($t = 0$)

which could indicate the mobilization of Fe from this mineral under certain conditions.

The Mn-dominant phases are Mn^{2+} and $MnSO_4$ (Table 7), whereas pyrolusite and rhodochrosite are clearly undersaturated in all of the leachates (Table 8), which suggests the mobilization of Mn from these minerals, but does not explain their immobilization in the soil experiments.

The most abundant species of Pb are $PbCO_3$, Pb^{2+} , and $PbSO_4$ (Table 7), and the leachates are undersaturated with respect to anglesite and cerrusite (Table 8). The Zn species calculated by PHREEQC are dominated by Zn^{2+} , $ZnSO_4$, and $ZnCO_3$ (Table 7), and the saturation indices showed that goslarite and zincosite are undersaturated (Table 8). Calcite is near equilibrium in the soil-column experiments (Table 8), as was seen by Blowes and Ptacek (1994), who observed near equilibrium conditions with calcite and siderite solubility in tailings pore water.

We used inverse modeling in the PHREEQC code to evaluate mass transfer in the column experiments (Parkhurst and Appelo 1999). Inverse modeling using the PHREEQC program is a geochemical mole-balance model that uses a set of defined minerals and, optionally, gases, that are related to an entry and output solution that account for the hydrogeochemical differences in the flow path. Inverse modeling has previously been applied to environmental problems associated with mining (Armienta et al. 2001; Eary et al. 2003; Navarro et al. 2006a, b) and in interpreting the geochemical properties of aquifers (Mahlknecht et al. 2004). Inverse modeling using observed mineral assemblages and mineral inferred from PHREEQC, can reveal the roles of mineral dissolution and precipitation (Seal et al. 2008). In applying inverse modeling to the column experiments, we took into account the main assumptions that may limit use of the approach (Alpers and Nordstrom 1999; Zhu and Anderson 2002).

Hydrogeochemical analyses of the first flush in the pure tailing leaching and soil column experiments with LMW were used to evaluate possible mass-transfer between the mine waste and soil. Potential phases in the inverse modeling were selected using calculated data of saturation indices derived from the PHREEQC and MINTEQ database, mineralogical observations of the material tailings, mining wastes, and alluvial soils, and direct observations in the dumping area. Thus, carbonate minerals, such as calcite, dolomite, cerrusite and siderite, sulphates, such as gypsum, jarosite and melanterite, and oxyhydroxides such as ferrihydrite, were included. The inclusion of pyrolusite, rhodochrosite, and zincosite, which are detected in the nearby mining area of Las Herrerías (Navarro and Cardellach 2008), was found to be needed to evaluate the theoretical role of these phases in the mobility of Mn and Zn, although they were not detected in the mineralogical study.

We also included halite and hematite since they were present in the tailings dump area. The MINTEQ thermodynamic database was used for the chemical equilibrium calculations. Table 9 shows the mineral phases used in the inverse modeling; Table 10 shows the models and molar transfers calculated using PHREEQC.

The results of inverse modeling showed the possible dissolution of calcite and gypsum, which may explain the increase of Ca^{2+} in the leachates and the neutralizing effect of alluvial soil in all the experiments. In order to better evaluate the calcite and gypsum dissolution, we constructed plots of Ca^{2+} and Mg^{2+} against HCO^{3-} and $SO_4{}^{2-}$ (Figs. 11, 12) using the hydrogeochemical data of soil column experiments with the LMW and saline solution. Figure 11 shows the relationship between the molar concentrations of Ca and Mg and the sum of sulphate and half of the bicarbonate concentrations. The data in Fig. 11 and the leachate hydrogeochemistry indicates that observed increases in Ca, Mg, HCO^{3-} and $SO_4{}^{2-}$ were the result of a simple dissolution of calcite, dolomite or Mg-calcite and gypsum. The data in Fig. 11 show a linear relation with a

Table 9 Mineral phases used in the inverse modeling

Mineral	Reaction	Log K (Minteq)
Calcite	$CaCO_3 = Ca^{2+} + CO_3{}^{2-}$	−8.47
Dolomite	$CaMg(CO_3)^2 = Ca^{2+} + Mg^{2+}\ CO_3{}^{2-}$	−17.0
Jarosite-K	$KFe_3(SO_4)_2(OH)_6 + 6H^+ = K^+ + 3Fe^{3+} + 2SO_4{}^{2-} + 6H_2O$	−14.8
Gypsum	$CaSO_4 \cdot 2H_2O = Ca^{2+} + SO_4{}^{2-} + 2H_2O$	−4.58
Halite	$NaCl = Na^+ + Cl^-$	1.582
Cerrusite	$PbCO_3 = Pb^{2+} + CO_3{}^{2-}$	−13.13
Melanterite	$FeSO_4 \cdot 7H_2O = Fe^{2+} + SO_4{}^{2-} + 7H_2O$	−2.209
Ferrihydrite	$Fe(OH)_3 + 3H+ = Fe^{3+} + 3H_2O$	4.891
Pyrolusite	$MnO^2 + 4H^+ + e^- = Mn^{3+} + 2H_2O$	15.861
Rhodochrosite	$MnCO_3 = Mn^{2+} + CO_3{}^{2-}$	−10.58
Zincosite	$ZnSO_4 = Zn^{2+} + SO_4{}^{2-}$	3.929
Hematite	$Fe_2O_3 + 6H^+ = 2Fe^{3+} + 3H_2O$	−4.008
Galena	$PbS + H^+ = Pb^{2+} + HS^-$	−13.97

Table 10 Models and molar transfers calculated by PHREEQC

Mineral	M1	M2	M3	M4	M5	M6	M7	M8
Calcite			2.18e + 00	2.22e + 00		1.90e − 03	1.93e − 03	
Dolomite	−2.50e − 02	−2.46e − 02	−2.50e – 02	−2.58e − 02	−2.58e − 02	−2.50e − 02	−2.58e − 02	−2.39e − 02
Gypsum	1.90e − 03		−2.17e + 00	−2.22e + 00	1.93e − 03			
Jarosite-K	−3.25e − 03	−3.33e − 03	−3.25e – 03	−3.33e − 03	−3.33e − 03	−3.25e − 03	−3.33e − 03	−3.25e − 03
Halite	4.74e − 04		4.74e – 04			4.74e − 04		4.74e − 04
Cerrusite	−1.90e + 00	−1.94e + 00	−2.14e + 00	−2.18e + 00	−1.94e + 00	−1.90e + 00	−1.94e + 00	−1.90e + 00
Melanterite	−1.93e + 00	−1.97e + 00			−1.97e + 00	−1.93e + 00	−1.97e + 00	−1.93e + 00
Ferrihydrite	−4.34e + 02	−4.46e + 02	−4.40e + 02	−4.50e + 02	−4.44e + 02	−4.34e + 02	−4.44e + 02	−4.34e + 02
Pyrolusite	6.63e + 00	6.77e + 00	8.57e + 00	8.74e + 00	6.76e + 00	6.63e + 00	6.77e + 00	6.63e + 00
Rhodochrosite	−6.63e + 00	−6.77e + 00	−8.57e + 00	−8.75e + 00	−6.77e + 00	−6.63e + 00	−6.77e + 00	−6.63e + 00
Zincosite	−1.77e − 04	−1.80e − 04	−1.77e − 04	−1.80e − 04	−1.80e − 04	−1.77e − 04	−1.80e − 04	−1.77e − 04
Hematite	2.18e + 02	2.23e + 02	2.20e + 02	2.25e + 02	2.23e + 02	2.18e + 02	2.23e + 02	2.18e + 02
Galena	1.90e + 00	1.94e + 00	2.14e + 00	2.18e + 00	1.94e + 00	1.90e + 00	1.94e + 00	1.90e + 00

Negative values indicate precipitation and positive values indicate dissolution

good coefficient of correlation ($R^2 = 0.9756$) and an intercept near zero. Since the ionic concentrations fall below the theoretical 1:1 line, the slope of the trend suggests that there is a partial loss of Ca and Mg, possibly due to cation exchange.

The soil experiment with the saline solution (Fig. 12) also showed the possible dissolution of calcite, Mg-calcite, gypsum, and release of additional Ca–Mg by cation exchange, because the samples are located above the theoretical equilibrium line with a slope of 1:1. In fact, carbonate minerals have an indirect influence on trace-element concentrations by neutralizing metal rich leachates, leading to adsorption and co-precipitation of metals with Fe^{3+} and Al oxyhydroxides and sulphates (Al et al. 2000). Thus, since Pb has a strong affinity to adsorb onto oxyhydroxides and hydrosulfates of Fe^{3+} (Gunsinger et al. 2006), which is saturated in the leachates, their precipitation may remove this metal.

Likewise, Zn mobility in near-neutral environments is limited because it is readily adsorbed by oxide, hydroxides, and aluminosilicates (Alvarez-Ayuso and Garcia-Sanchez 2003). Nevertheless, it can form organic complexes in slightly alkaline soils, and hydroxianions in highly alkaline environments, increasing its solubility in both cases. High Zn concentrations in ground water and soils are usually related to desorption or dissolution of ferrihydrite (Jurjovec et al. 2002).

The results of inverse modeling also showed that the removal of Mn, Pb, and Zn in the soil leaching experiments may be theoretically caused by the precipitation of rhodochrosite, cerrusite, and zincosite, although these minerals have not been detected in the XRD mineral analysis

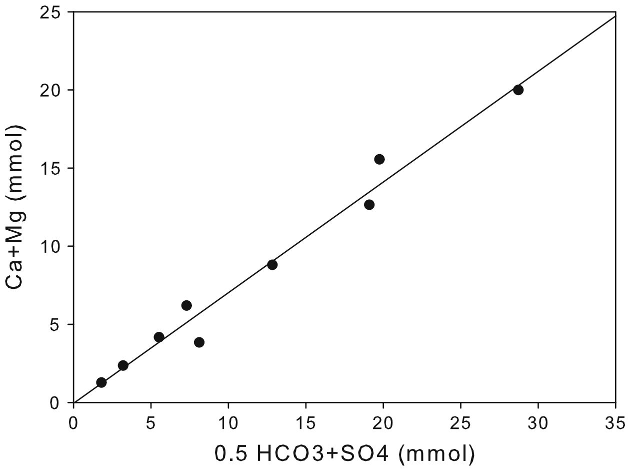

Fig. 11 Plot of $Ca^{2+} + Mg^{2+}$ versus 0.5 HCO^{3-} + SO_4^{2-} from the experiment of leaching of mine waste and alluvial soil with LMW

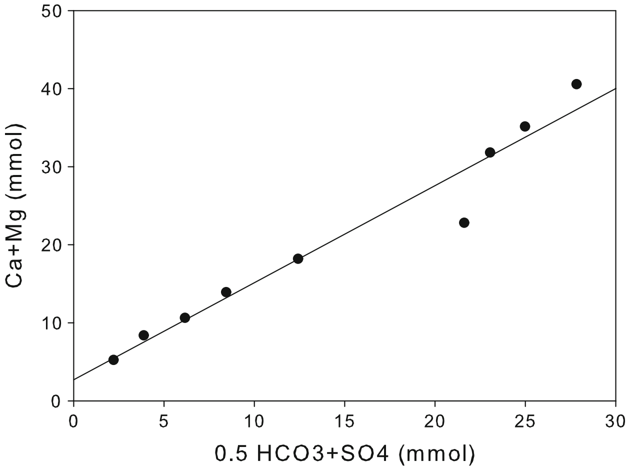

Fig. 12 Plot of $Ca^{2+} + Mg^{2+}$ versus 0.5 HCO^{3-} + SO_4^{2-} from the experiment of leaching of mine waste and alluvial soil with saline solution

performed (Table 1). This result is consistent with the pH-Eh speciation diagrams for Pb and Zn in the presence of sulfur (Stumm and Morgan 1995). The Pb diagram showed that cerrusite is the most stable mineral phase under the pH-Eh conditions in the soil leaching experiments, which agrees with the model calculated using the PHREEQC code. The pH-Eh diagram of Zn shows that zincosite ($ZnSO_4$) and smithsonite ($ZnCO_3$) are the most stable species under the experimental soil leaching conditions.

The removal of Mn may be theoretically associated with the stability of $MnCO_3$ in the column-experiment conditions, although pyrolusite and rhodochrosite were undersaturated in all of the leachates (Table 8). However, in some cases, such as aquifer environments, Mn^{2+} may be reoxidized and precipitated as MnO_2 (Postma and Appelo 2000). Besides, Mn may be attenuated by coprecipitation and adsorption with goethite and jarosite (McGregor et al. 1998), species which are saturated in the leachate conditions (Table 8).

The conditions of the soil column leachates are similar to the pH-Eh values of neutral water observed downstream of the acid and transition zones in aquifers contaminated by AMD. There, ground water contains high levels of Ca, Fe, and sulfates, as observed in the leachates.

Conclusions

The uncontrolled dumped tailings of the El Arteal deposit in the Sierra Almagrera mining area (Almería, SE Spain) had high amounts of Ag (26.6 ppm), As (278.4 ppm), Ba (5.8 wt%), Cu (59.0 ppm), Pb (2879.3 ppm), Sb (169.8 ppm), and Zn (2179.2 ppm). The contaminants of greatest environmental concern are As and Pb, which present a mean concentration of 278.4 and 2879.3 ppm, and as high as 460 and 5,428 ppm, respectively. The values detected in the soils and sediment surrounding the tailings impoundment, which is an area of intense agricultural activity, were 340 and 3,244 ppm, respectively.

The oxidation of sulfides and sulfosalts in the tailings deposit of El Arteal resulted in the precipitation of secondary phases: jarosite ($KFe_3(SO_4)_2(OH)_6$), argentojarosite ($Ag_2Fe_6(SO_4)_4(OH)_{12}$), crystalline oxyhydroxide of Fe (goethite), amorphous ferric hydroxide (Fe $(OH)_3$), clay minerals, natroalunite ($NaAl_3(SO_4)_2(OH)_6$), gypsum ($CaSO_4 \cdot 2H_2O$), and efflorescent salts. The dissolution and precipitation of these minerals may control the metal release from the tailings.

In the laboratory column experiments, Al, Ba, Cd, Cu, Fe, Mn, Ni, Pb, Sr, and Zn all leached from the tailings. However, when the leachate passed through the soil, Al, Ba, Cd, Cu, Mn, Pb, and Zn were retained, while Fe and Sr were clearly mobilized. The immobilization of metals in the alluvial soils studied is most likely due to the increase in pH caused by calcite dissolution. The models also pointed to this possibility (Table 10). Thus, carbonate minerals may have an indirect influence on trace-element concentrations by neutralizing metal rich leachates, leading to adsorption and co-precipitation of metals with ferric and Al oxyhydroxides and sulphates. The result may be a set of attenuation processes associated with metal coprecipitation and adsorption with goethite and jarosite, which are saturated in the leachate conditions (Table 8).

The results of inverse modeling showed that the removal of Mn, Pb, and Zn in the soil leaching experiments may be theoretically caused by the precipitation of rhodochrosite, cerrusite, and zincosite. Under the pH-Eh conditions in the soil-leaching experiments, cerrusite is the most stable mineral phase, which is concordant with the model calculated using the PHREEQC code. Also, zincosite ($ZnSO_4$), smithsonite ($ZnCO_3$), and rhodochrosite ($MnCO_3$) are the most stable species under the experimental soil leaching conditions.

The sorption of some metals (Cu, Pb, and Zn) onto oxyhydroxides of Al and Mn, clay materials, and organic matter may also explain the removal of these metals from the tailings leachates. These experimental results suggest that natural soils can act as reactive barriers at mine sites, controlling metal mobilization by several attenuation processes.

Acknowledgments Financial support was provided through an agreement between the Technical University of Catalonia (UPC) and the private sector (Project C-7300). Funding was also received from the Spanish Ministry of Science and Technology (Projects REN2003-09247-C04-03 and ENE2006-13267-C05-03), in collaboration with the Research Center for Energy, Environment and Technology (CIEMAT).

References

Al TA, Martin CJ, Blowes DW (2000) Carbonate-mineral/water interactions in sulfide-rich mine tailings. Geochim Cosmochim Acta 64:3933–3948

Alakangas L, Öhlander B (2006) Pilot-scale studies of different covers on unoxidised sulphide-rich tailings in Nothern Sweeden: the geochemistry of leachate waters. Mine Water Environ 25:171–183

Almagro Gorbea M (1970) Las fechas del C-14 para la prehistoria y la arqueología peninsular. Trabajos de Prehistoria 27:9–43

Alpers CN, Nordstrom DK (1999) Geochemical modeling of water-rock interactions in mining environments. In: Plumlee GS, Logson MJ (eds) The environmental geochemistry of mineral deposits. Rev Econ Geol 6A:289–323

Alvarez-Ayuso E, Garcia-Sanchez A (2003) Palygorskite as a feasible amendment to stabilize heavy metal polluted soils. Environ Pollut 125:337–344

Armienta MA, Villaseñor G, Rodríguez R, Ongley LK, Mango H (2001) The role of arsenic-bearing rocks in groundwater pollution at Zimapán Valley, México. Environ Geol 40:571–581

Arribas A Jr, Cunningham CG, Rytuba JJ, Rye RO, Kelly WC, Podwysecki MH, McKee EH, Tosdal RM (1995) Geology, geochronology, fluid inclusions, and isotope geochemistry of the Rodalquilar gold alunite deposit, Spain. Econ Geol 90:795–822

Balistrieri LS, Box SE, Bookstrom AA (2002) A geoenvironmental model for polymetallic vein deposits: a case study in the Coeur d′Alene mining district and comparisons with drainage from mineralized deposits in the Colorado Mineral Belt and Humboldt Basin, Nevada. USGS open file report 02-195, pp 143–160

Basta NT, McGowen SL (2004) Evaluation of chemical immobilization treatments for reducing heavy metal transport in a smelter-contaminated soil. Environ Pollut 127:73–82

Blowes DW, Ptacek CJ (1994) Acid-neutralization mechanisms in inactive mine tailings. In: Jambor JL, Blowes DW (eds) The environmental geochemistry of sulfide mine-wastes. Mineralogical association of Canada short course handbook 22, pp 271–292

Blowes DW, Jambor JL, Hanton-Fong CJ (1998) Geochemical, mineralogical and microbiological characterization of a sulphide-bearing carbonate-rich gold-mine tailings impoundment, Jouetl, Québec. Appl Geochem 13:687–705

Breeuwsma A, Wösten JHM, Vleeshouwer JJ, Van Slobbe AM, Bouma J (1986) Derivation of land qualities to assess environmental problems from soil surveys. Soil Sci Soc Am J 50:186–190

Cidu R, Biddau R, Fanfani L (2008) Impact of past mining activity on the quality of groundwater in SW Sardinia (Italy). J Geochem Explor 2–3:125–132

Cravotta CA III, Watzlaf JB (2002) Design and performance of limestone drains to increase pH and remove dissolved metals from acidic mine drainage. In: Naft DL, Morrison SJ, Fuller CC, Davis JA (eds) Handbook of groundwater remediation using permeable reactive barriers—application to radionuclides, trace metals, and nutrients. Academic Press, San Diego, pp 19–66

Dybowska A, Farago M, Valsani-Jones E, Thornton I (2006) Remediation strategies for historical mining and smelting sites. Sci Progress 89:71–138

Dzomback DA, Morel FMM (1990) Surface complexation modeling: hydrous ferric oxide. Wiley, New York 393 pp

Eary LE, Runnels DD, Esposito KJ (2003) Geochemical controls on groundwater composition at the Cripple Creek Mining District, Colorado. Appl Geochem 18:1–24

EPA (US Environmental Protection Agency) (2007) Monitored natural attenuation of inorganic contaminants in groundwater. EPA/600/R-07/140, vol 2

Ford RG, Wilkin RT, Puls RW (2007) Monitored natural attenuation of inorganic contaminants in ground water. EPA/600/R-07/140, vol 2. Cincinnati

Frau F, Ardau C, Fanfani L (2008) Environmental geochemistry and mineralogy of lead at the old mine area of Baccu Locci (south-east Sardinia, Italy). J Geochem Explor 2–3:105–115

Gunsinger MR, Ptacek CJ, Blowes DW, Jambor JL, Moncur MC (2006) Mechanisms controlling acid neutralization and metal mobility within a Ni-rich tailings impoundment. Appl Geochem 21:1301–1321

Heikkinen PM, Räisänen ML, Johnson RH (2009) Geochemical characterization of seepage and drainage water quality from two sulphide mine tailings impoundments: acid mine drainage versus neutral mine drainage. Mine Water Environ 28:30–49

Hulshof AHM, Blowes DW, Gould WD (2006) Evaluation of in situ layers for treatment of acid mine drainage: a field comparison. Water Res 40:1816–1826

Jambor JL, Nordstrom DK, Alpers CN (2000) Metal-sulfate salts from sulfide mineral oxidation. In: Alpers CN, Jambor JL, Nordstrom DK (eds) Sulfate minerals—crystallography, geochemistry, and environmental significance. Mineralogical Society of America. Rev Mineral Geochem 40:303–350

Jurjovec J, Ptacek CJ, Blowes DW (2002) Acid neutralization mechanisms and metal release in mine tailings: a laboratory column experiment. Geochim Cosmochim Acta 66:1511–1523

Kovács E, Dubbin WE, Tamás J (2006) Influence of hydrology on heavy metal speciation and mobility in a Pb-Zn mine tailings. Environ Pollut 141:310–320

Kumpiene J, Lagerkvist A, Maurice C (2007) Stabilization of Pb- and Cu-contaminated soil using coal fly ash and peat. Environ Pollut 145:365–373

Mahlknecht J, Schneider JF, Merkel BJ, Navarro de León I, Bernasconi SM (2004) Groundwater recharge in a sedimentary basin in semi-arid México. Hydrogeol J 12:511–530

McCullough CD, Lund MA, May JM (2008) Field-scale demonstration of the potential for sewage to remediate acidic mine wastes. Mine Water Environ 27:31–39

McGregor RG, Blowes DW, Jambor JL, Robertson WD (1998) The solid-phase controls on the mobility of heavy metals at the Copper Cliff tailings area, Sudbury, Ontario, Canada. J Contam Hydrol 33:247–271

Moreno T, Oldroyd A, McDonald I, Gibbons W (2007) Preferential fractionation of trace metals-metalloids into PM10 resuspended from contaminated gold mine tailings at Rodalquilar, Spain. Water Air Soil Poll 179:93–105

Navarro A, Cardellach E (2008) Mobilization of Ag, heavy metals and Eu from the waste deposit of Las Herrerías mine (Almería, SE Spain). Environ Geol 56:1389–1401

Navarro A, Martínez F (2008) Effects of sewage sludge application on heavy metal leaching from mine tailings impoundments. Bioresour Technol 99:7521–7530

Navarro A, Martínez J, Font X, Viladevall M (2000) Modeling of modern mercury vapor transport in an ancient hydrothermal system: environmental and geochemical implications. Appl Geochem 15:281–294

Navarro A, Collado D, Carbonell M, Sánchez JA (2004) Impact of mining activities in a semi-arid environment: Sierra Almagrera district, SE Spain. Environ Geochem Health 26:383–393

Navarro A, Chimenos JM, Muntaner D, Fernández I (2006a) Permeable reactive barriers for the removal of heavy metals: lab-scale experiments with low-grade magnesium oxide. Ground Water Monitor Remed 26:142–152

Navarro A, Biester H, Mendoza JL, Cardellach E (2006b) Mercury speciation and mobilization in contaminated soils of the Valle del Azogue Hg mine (SE, Spain). Environ Geol 49:1089–1101

Navarro A, Cardellach E, Mendoza JL, Corbella M, Domènech LM (2008) Metal mobilization from base-metal smelting slag dumps in Sierra Almagrera (Almería, Spain). Appl Geochem 23:895–913

Nicholson RV, Gillham RW, Reardon EJ (1988) Pyrite oxidation in carbonate-buffered solution: 1. Experimental kinetics. Geochim Cosmochim Acta 52:1077–1085

Nicholson RV, Gillham RW, Reardon EJ (1990) Pyrite oxidation in carbonate-buffered solution: 2. Rate control by oxide coatings. Geochim Cosmochim Acta 54:395–402

Oen IS, Fernández JC, Manteca JI (1975) The lead-zinc and associated ores of La Unión Sierra de Cartagena, Spain. Economic Geol 70:1259–1278

Ogata A, Banks RB (1961) A solution of the differential equation of longitudinal dispersion in porous media. USGS professional paper 411-A, 7 pp

Parkhurst DL, Appelo CAJ (1999) User′s Guide to PHREEQC (version 2)—a computer program for speciation, batch-reaction, one-dimensional transport, and inverse geochemical calculations, USGS water-resources investigations report 99-4259, 312 pp

Pérez-López R, Nieto JM, Ruiz de Almodóvar G (2007) Immobilization of toxic elements in mine residues derived from mining activities in the Iberian Pyrite Belt (SW Spain): laboratory experiments. Appl Geochem 22:1919–1935

Plumlee GS, Smith KS, Montour MR, Ficklin WH, Mosier EL (1999) Geologic controls on the composition of natural waters and mine waters. In: Filipek LH, Plumlee GS (eds) The environmental geochemistry of mineral deposits. Reviews in economic geology, vol 6B. Chelsea, pp 373–432

Postma D, Appelo CAJ (2000) Reduction of Mn-oxides by ferrous iron in a flow system: column experiment and reactive transport modeling. Geochim Cosmochim Acta 64:1237–1247

Ribet I, Ptacek CJ, Blowes DW, Jambor JL (1995) The potential for metal release by reductive dissolution of weathered mine tailings. J Contam Hydrol 17:239–273

Robles-Arenas VM, Rodríguez R, García C, Manteca JI, Candela L (2006) Sulphide-mining impacts in the physical environment: Sierra de Cartagena-La Unión (SE Spain) case study. Environ Geol 51:47–64

Romero FM, Armienta MA, González-Hernández JL (2007) Solid-phase control on the mobility of potentially toxic elements in an abandoned lead/zinc mine tailings impoundment, Taxco, Mexico. Appl Geochem 22:109–127

Seal RR, Hammarstrom JM, Johnson AN, Piatak NM, Wandless GA (2008) Environmental geochemistry of a Kuroko-type massive sulfide deposit at the abandoned Valzinco mine, Virginia, USA. Appl Geochem 23:320–342

Silliman SE, Simpson ES (1987) Laboratory evidence of the scale effect in dispersion of solutes in porous media. Water Resour Res 23:1667–1673

Smuda J, Dold B, Friese K (2007) Mineralogical and geochemical study of element mobility at the sulfide-rich Excelsior waste rock dump from the polymetallic Zn-Pb-(Ag-Bi-Cu) deposit, Cerro de Pasco, Peru. J Geochem Expl 92:97–110

Sneddon IR, Orueetxebarria M, Hodson ME, Schofield PF, Valsami-Jones E (2006) Use of bone meal amendments to immobilize Pb, Zn and Cd in soil: a leaching column study. Environ Pollut 144:816–825

Stumm W, Morgan JJ (1995) Aquatic chemistry: chemical equilibria and rates in natural waters. Wiley, New York 1022 pp

Talavera O, Armienta A, García J, Flores N (2006) Geochemistry of leachates from the El Fraile sulfide tailings piles in Taxco, Guerrero, southern Mexico. Environ Geochem Health 28:243–255

Wilkin RT (2008) Contaminant attenuation processes at mine sites. Mine Water Environ 27:251–258

Wray DS (1998) The impact of unconfined mine tailings and anthropogenic pollution on a semi-arid environment: an initial study of the Rodalquilar mining district, southeast Spain. Environ Geochem Health 20:29–38

Yanful EK, Simms PH, Payant SC (1999) Soil covers for controlling acid generation in mine tailings: a laboratory evaluation of the physics and geochemistry. Water Air Soil Poll 114:347–375

Younger PL, Banwart SA, Hedin RS (2002) Mine water hydrology, pollution, remediation. Kluwer, Dordrecht 442 pp

Zhu C, Anderson G (2002) Environmental applications of geochemical modeling. Cambridge University Press, Cambridge 284 pp